RSC Advances

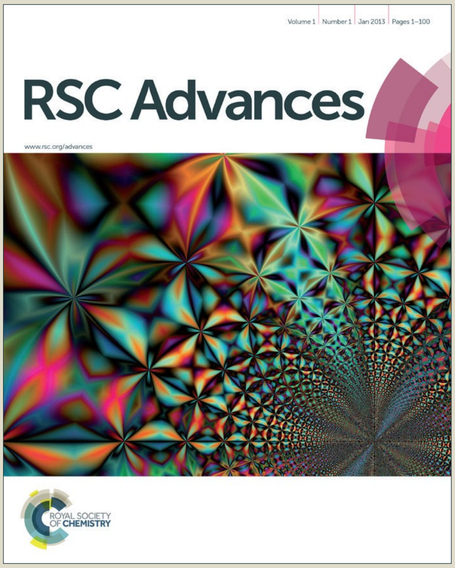

ROYAL SOCIETY OF CHEMISTRY

www.rsc.org/advances

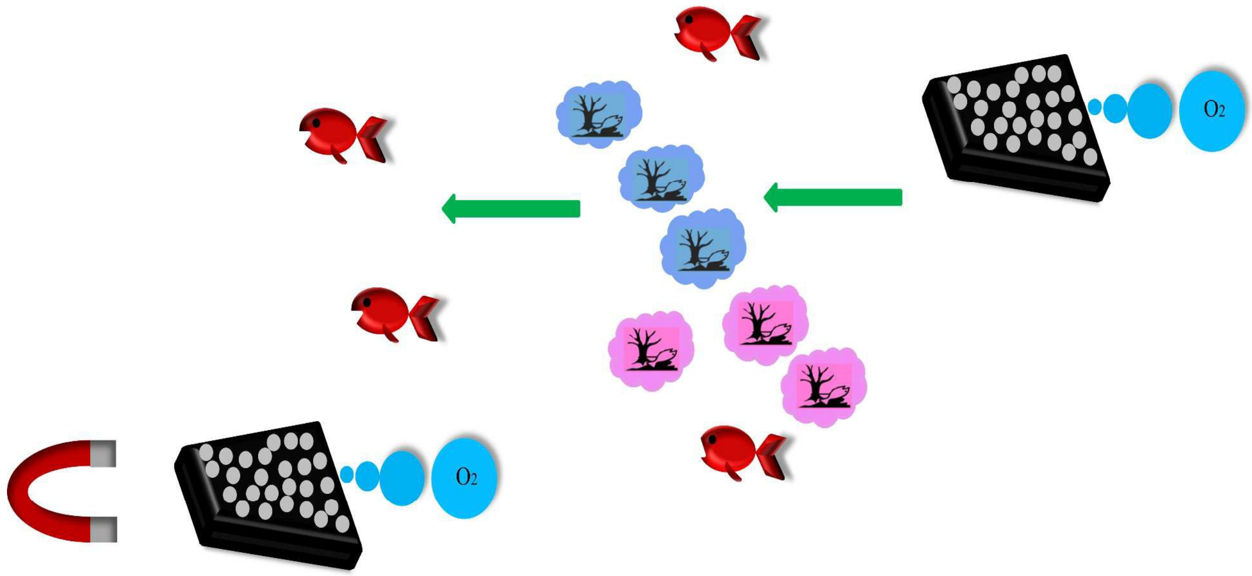
O2
O2

A simple method for fabrication of nanomotor based on gold nano sheet decorated with CoPt nanoparticles†

Mahmoud Amouzadeh Tabrizi, Mojtaba Shamsipur*

Received (in XXX, XXX) Xth XXXXXXXXX 200X, Accepted Xth XXXXXXXXX 200X
First published on the web Xth XXXXXXXXX 200X
DOI: 10.1039/b000000x

In this communication, we present an extremely rapid, simple and template-less method for fabrication of CoPt/gold nanosheet motors (NSMs) electrochemically, via a three-steps applied potential process. The oxygen-propelled NSMs can be guided by a magnetic force in an aquieous solution containing 1% hydrogen peroxide as fuel. Finally, the catalytic activity of the prepared NSMs in the degradation of rhodamin B (RB) and methylene blue (MB) were investigated as models for environmental remediation.

Catalytic nanomotors, first discovered by Mallouk and Sen in 2004[1], are nanoscale manufactural devices which can be propelled by different mechanisms[2, 3]. In recent years, increasing number of researches in field of nanoscience have been devoted to the synthesis of nanomators, opening the door for new applications in nanotechnology, including drug delivery[4-7], surgery[8-10], bio-isolation[11-14], chemical sensing[15-17] and environmental remediation[18-21]. Up to now, various methods have been reported for synthesis of nanomotors[22-26]. However, the fabrication process of these methods (especially template based [1, 4, 17, 22, 25-26] and rolled-up based methods [8, 27-29]) are generally time-consuming, expensive and need to operators with high experience. Therefore, search for effective, low-cost and simple methods for synthesis of nanomotors is still desirable.

Herein, for the first time, we report a simple and rapid method for fabrication of oxygen-propelled magnetically-guided CoPt/gold nanosheet motors which they have non-uniform structure. Furthermore, we exploited that the fabricated nanomotors, in the presence of 1% hydrogen peroxide as fuel, can be magentically guided to pollution regions for degradation of organic pollutants such as rhodamin B (RB) and methylene blue (MB).

The characterization of NSMs was examined by scanning electron microscopy (SEM) and scanning electron microscopy with energy dispersive X-ray spectroscopy (SEM/EDX). The obtained images are shown in Fig. 1. It can be seen that the prepared NSMs possess a sheet structure of gold, upon which are deposited the CoPt alloy nanoparticles (Fig. 1 A, B and C). However, it can be seen that the propertied NSMs have different structures with each other. The average thickness of the gold nanosheet was approximately ~70 nm, the average size of deposited CoPt alloy nanoparticles is approximately ~ 35 nm. Also, the elemental analysis of obtained NSMs was carried out by EDX and the results are shown in Fig. 1D. The EDX results clearly indicated that the prepared NSMs contain 93.31 wt% gold, 4.64 wt% cobalt and 2.05 wt% platinum. Fig. S1 also shows the typical SEM image of gold nanosheet film.

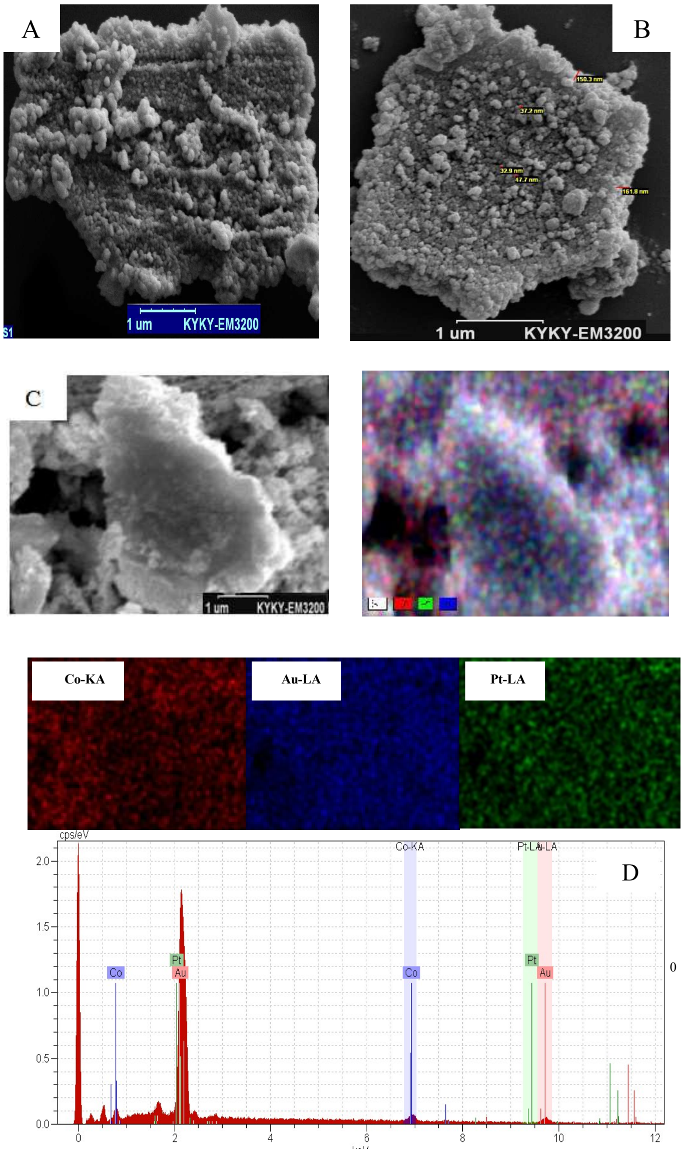

Fig.1. FE-SEM (A,B) and SEM/EDX (C) images of perperated NSMs, (D) EDX spectra obtained for NSMs.

Remote control of nanomotor is a very important aspect. In this work, the prepared NSM was guided in a solution by a magnetic force. Fig. 2 shows a series of optical images demonstrating the rout of the NSM in a solution containing 1% hydrogen peroxide as a fuel, via a magnetically guided movement, with the elapse of time (from A to F, in a duration of about 3 s). The corresponding movie is shown in the supporting information as video S1 and video S2. As shown in these videos, the production of oxygen-bubbles from surface of NSMs led to its movement in solution (video S1, Fig 2 A, B, C). After applying an external magnet force, the NSM are also quickly moved toward magnetic direction (Video S1, Fig 2 D, E, F).

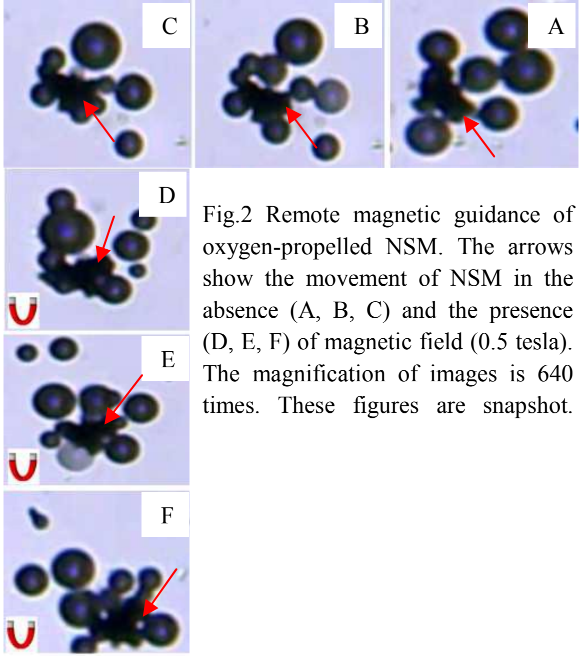

Fig.2 Remote magnetic guidance of oxygen-propelled NSM. The arrows show the movement of NSM in the absence (A, B, C) and the presence (D, E, F) of magnetic field (0.5 tesla). The magnification of images is 640 times. These figures are snapshot.

Fig. 3 displays the schematically the oxygen-bubble-propelled magnetically-guided movement of the NSMs. The presence of CoPt magnetic nanoparticles not only results in catalytic decomposition of H_2O_2 to oxygen bubble, which makes the movement of NSMs possible, but also allow the remote control of NSMs with a magnetic field.

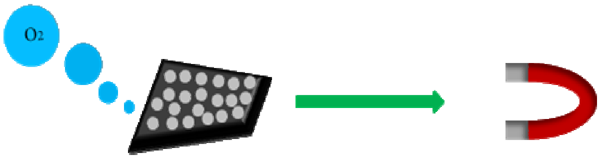

Fig.3 Schematics of movement of oxygen-propelled magnetically-guided NSM.

The time-lapse images in Fig. S2, captured from Video S3, display the move of oxygen-propelled NSM under the irradiation of a focused NIR laser in 0.1% (v/v) H_2O_2. It can be seen that the increase in temperature surrounding the NSM due to NIR irradiation rapidly induces higher rates of catalytic decomposition of H_2O_2 to O_2, producing oxygen bubbles and propulsion force to move of NSM accordingly. It should be noted that in absence of the irradiation of a focused NIR laser, the catalytic decomposition rate of H_2O_2 is too low to power self-propulsion of the NSM at this concentration level.

With the aim of investigating of the catalytic performance of the prepared NSMs toward the degradation of organic pollutants, we selected RB and MB as models for environmental remediation in presence of 1% hydrogen peroxide and 0.1M NaOH as a peroxide activator with no external stirring. After the guiding the NSMs to polluted region by a magnetic force, the color of solution containing of RB and MB decreased rapidly (see, Fig. S3A, EIS for RB and Fig. S3B, EIS for MB), due to the catalytic property of the prepared NSMs in degradation process of the organic water pollutants components. Based on previous report, pt nanoparticles along with the H_2O_2 and peroxide activator generate HOO• radicals which degrade organic pollutants[30]. Also, the movement of the NSMs and their bubble generation contribute to the substantial fluid motion and to the accelerated decontamination process. The changes in the absorption spectra of RB at 554 nm and MB at 656 nm in aqueous solution exposed to NSMs in the presence of hydrogen peroxide are also shown in Figs. 4A and 4B, respectively. It can be seen that the absorption spectra of RB and MB are completely disappeared after degradation by NSMs, over a time period of 2h. But in the absence of the NSMs, no appreciable degradation of the RB and MB solutions were observed after 2 h (Fig. S4). Also, in absence of magnetic filed the NSM could not receive to pollution region after 2 h (Fig. S5).

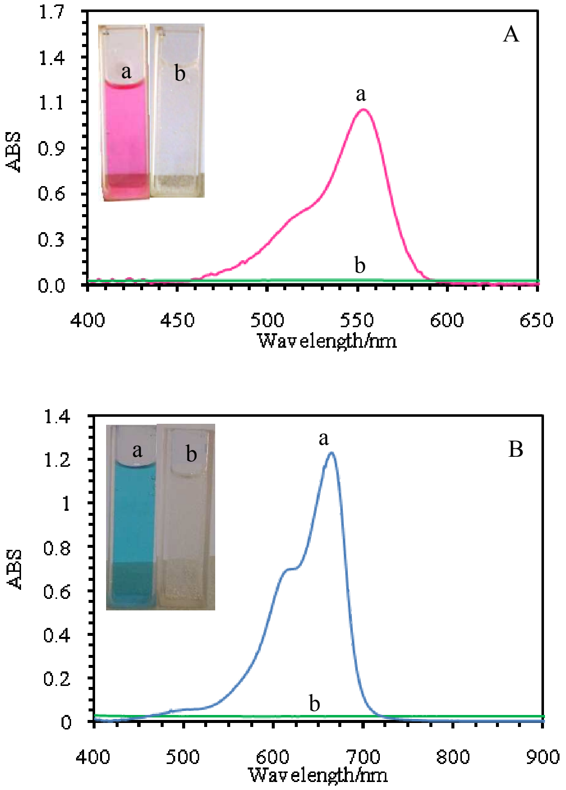

Fig.4 UV–Vis absorption spectra of 60 ppm of RB (A) and MB (B), before (a) and after (b) degradation by NSMs. The inset shows the visual color changes of the RB (A) and MB (B) before (a) and after (b) degradation.

Conclusions

This study describes a rapid and simple method fabrication of nanomotor. The prepared nanomotor (NSMs) can be moved by catalytic oxidation of hydrogen peroxide to oxygen bubbles. Due to the magnetic and catalytic properties of CoPt nanoparticles present, the NSMs can be used for their guided movement to the polluted region of water and subsequent degradation of the corresponding pollutants. We really belief that the proposed nanomotor system could provide a unique opportunity for researchers to apply them in a wide fields of nanotechnology, such as environmental remediation, drug delivery, surgery, bio-isolation, chemical and bio-sensing and etc.

Experimental section

Synthesis of CoPt/gold nanosheet motors

First, the surface of a gold disk electrode (3.0 mm diameter) was polished successively using 0.3, 0.1 and 0.05 µm alumina slurry, respectively, and then cleaned in ethanol and water, under ultra-sonication. The freshly polished gold electrode was anodized at 6 V (versus Ag|AgCl|saturated KCl) in 0.5 M phosphate buffer (PB) solution of pH 7.0 for 20 min and then reduced at -0.3 V for 5 min to obtain the gold nano film. Subsequently, the gold nanofilm electrode was immersed in a solution of 1 M NH_4Cl+ 0.1 M H_3BO_3 at pH 4.5 containing 0.1 mM $CoCl_2$ and 0.02 mM Na_2PtCl_6 and, then, a -1.15 V potential was applied for 20 min. Finally, the obtained electrode was washed with water for 10 s, then immersed in doubly distilled water (2.0 mL) and sonicated for 5 min, in order to release the prepared CoPt/gold nanosheets with non-uniform structure into the solution. Also, in during the sonication process, the decorated nanofilm with CoPt nanoparticles will break to nanosheets with different structures. Finally, the solution was centrifuged at 2000 rpm for 5 min, the separated products for subsequent studies.

Apparatus

Scanning electron microscopy (SEM) was performed on a Philips instrument, Model XL-30 with an accelerating voltage of 26 kV. A neodymium (NdFeB) magnet (0.5 Tesla) was used for magnetically control of the movement of nanomotor. UV–visible absorption spectra were recorded using a single beam Agillan UV–vis spectrophotometer (model G1103A). The electrochemical experiments were performed using the µAutolab electrochemical system (Eco-Chemie, Utrecht, The Netherlands) equipped with GPES and FRA 4.9 software. A three-electrode assembled cell was employed, consisting of the gold disk electrode (3.0 mm diameter) as the working electrode, a platinum-wire as a counter electrode and a Ag|AgCl|saturated KCl electrode as the reference electrode. Optical microscope videos (Video S1, Video S2 and Video S3) and images (Fig.3 and Fig. S2) were obtained with an Olympus IX71 microscope coupled to digital camera Olympus DP72. The NSMs movement was tracked using Cellsens Olympus image software. The free software XiLi 3GP (video converter) was used to edit video. Near infrared (NIR) laser beam at 780 nm with a power of 200 mW has been used. All reagents were of analytical grade.

Notes and references

* *Department of Chemistry, Razi University, Kermanshah, Iran. Phone: (+98) 831-4274580. E-mail: mshamsipur@yahoo.com,*

† Electronic Supplementary Information (ESI) available: [Figs and videos]. See DOI: 10.1039/b000000x/

1. W. F. Paxton, K. C. Kistler, C. C. Olmeda, A. Sen, S. K. St. Angelo, Y. Cao, T. E. Mallouk, P. E. Lammert and V. H. Crespi, *J. Am. Chem. Soc,* 2004, 126, 13424–13431.
2. J. Wang and W. Gao, *ACS Nano*, 2012, 6, 5745–5751.
3. W. Wang, W. Duan, S. Ahmed, T. E. Mallouk and A. Sen, *Nano Today*, 2013, 8, 531–554.
4.W. Gao, D. Kagan, O. S. Pak, C. Clawson, S. Campuzano, E. Chuluun-Erdene, E. Shipton, E. E. Fullerton, L. Zhang, E. Lauga and J. Wang, *Small*, 2012, 8, 460–467.
5. D. Patra, S. Sengupta, W. Duan, H. Zhang, R. Pavlick and A. Sen, *Nanoscale*, 2013, 5, 1273–1283.
6. M. G. L. van den Heuvel and C. Dekker, *Science*, 2007, 317, 333-336.
7. D. Kagan, R. Laocharoensuk, M. Zimmerman, C. Clawson, S. Balasubramanian, D. Kang, D. Bishop, S. Sattayasamitsathit, L. Zhang and J. Wang, *Small*, 2010, 6, 2741–2747.
8. W. Xi, A. A. Solovev, A. N. Ananth, D. H. Gracias, S. Sanchez and O. G. Schmidt, *Nanoscale*, 2013, 5, 1294–1297.
9. A. A. Solovev, W. Xi, D. H. Gracias, S. M. Harazim, C. Deneke, S. Sanchez and O. G. Schmidt, *ACS Nano*, 2012, 6, 1751–1756.
10. D. Kagan, M. J. Benchimol, J. C. Claussen, E. Chuluun-Erdene, S. Esener and J. Wang, *Angew. Chem., Int. Ed*, 2012, 51, 7519–7521.
11. M. Garcia, J. Orozco, M. Guix, W. Gao, S. Sattayasamitsathit, A. Escarpa, A. Merkoci and J. Wang, *Nanoscale*, 2013, 5, 1325–1331.
12. S. Campuzano, J. Orozco, D. Kagan, M. Guix, W. Gao, S. Sattayasamitsathit, J. C. Claussen, A. M. i and J. Wang, *Nano Lett*, 2011, 12, 396−401.
13. S. Balasubramanian, D. Kagan, C.-M. J. Hu, S. Campuzano, M. J. L.-C. on, N. Lim, D. Y. Kang, M. Zimmerman, L. Zhang and J. Wang, *Angew. Chem., Int. Ed*, 2011, 50, 4161–4164.
14. J. Orozco, A. Cortes, G. Cheng, S. Sattayasamitsathit, W. Gao, X. Feng, Y. Shen and J. Wang, *J. Am. Chem. Soc*, 2013, 135, 5336–5339.
15. J. G. S. Moo, H. Wang, G. Zhao and M. Pumera, *Chem. Eur. J,* 2014, 20, 4292–4296.
16. E. S. Olson, J. Orozco, Z. Wu, C. D. Malone, B. Yi, W. Gao, M. Eghtedari, J. Wang and R. F. Mattrey, *Biomater*, 2013, 34, 8918–8924.
17. D. Kagan, P. Calvo-Marzal, S. Balasubramanian, S. Sattayasamitsathit, K. M. Manesh, G. U. Flechsig and J. Wang, *J. Am. Chem. Soc*, 2009, 131, 12082–12083.
18. L. Soler and S. Sanchez, *Nanoscale*, 2014, 6, 7175–7182.
19. W. Gao and J. Wang, *ACS Nano*, 2014, 8, 3170–3180.
20. W. Gao, X. Feng, A. Pei, Y. Gu, J. Li and J. Wang, *Nanoscale*, 2013, 5, 4696–4700.
21. M. Guix, J. Orozco, M. Garcı´a, W. Gao, S. Sattayasamitsathit, A. Merkoc-i, A. Escarpa and J. Wang, *ACS Nano*, 2012, 6, 4445–4451.
22. A. A. Solovev, Y. Mei, E. Bermúdez Ureña, G. Huang and O. G. Schmidt, *Small*, 2009, 5, 1688–1692.
23. W. Huang, M. Manjare and Y. Zhao, *J. Phys. Chem. C*, 2013, 117, 21590–21596.
24. W. Gao, A. Pei, R. Dong and J. Wang, *J. Am. Chem. Soc*, 2014, 136, 2276–2279.
25. D. A. Wilson, B. de Nijs, A. van Blaaderen, R. J. M. Nolte and J. C. M. van Hest, *Nanoscale*, 2013, 5, 1315–1318.
26. G. Zhao, A. Ambrosi and M. Pumera, *Nanoscale*, 2013, 5, 1319–1324.
27. S. Sanchez, A. A. Solovev, S. Schulze and O. G. Schmidt, *ChemComm*, 2011, 47, 698–700.
28. Y. F. Mei, G. S. Huang, A. A. Solovev, E. B. Urena, F. D. I. Monch, T. Reindl, R. K. Y. Fu, P. K. Chu and O. G. Schmidt, *Adv. Mater.*, 2008, 20, 4085-4090.
29. J. Li, J. Zhang, W. Gao, G. Huang, Z. Di, R. Liu, JosephWang and Y. Mei, *Adv. Mater.* , 2013, 25, 3715–3721.
30 . J. Orozco, G. Cheng, D. Vilela, S. Sattayasamitsathit, R. Vazquez-Duhalt, G. Valdés-Ramírez, O. S. Pak, A. Escarpa, C. Kan and J. Wang, *Angew. Chem., Int. Ed*, 2013, 52, 13276–13279.